J Fluoresc (2014) 24:417–424
DOI 10.1007/s10895-013-1307-6

ORIGINAL PAPER

9, 10-Bis(8-Quinolinoxymethyl)Anthracene—A Fluorescent Sensor for Nanomolar Detection of Cu^{2+} with Unusual Acid Stability of Cu^{2+}-Complex

Prabhpreet Singh · Rahul Kumar · Subodh Kumar

Received: 9 June 2013 / Accepted: 25 September 2013 / Published online: 11 October 2013

Abstract In this work, the dipod 9,10-bis(8-quinolinoxymethyl) anthracene (**1**) and for comparison, monopod 9-(8-quinolinoxymethyl)anthracene (**2**) have been synthesized. The fluoroionophore **1** in pH 7.1 HEPES buffered CH_3CN:H_2O (4:1 v/v) solution shows quenching only with Cu^{2+} with lowest limit of detection 150 nM, amongst various metal ions. Fluoroionophore **1** could also be applied to sense Co^{2+} with lowest limit of detection 600 nM. By modulating the pH of the solution and concentration of Cu^{2+}, **1** shows respective "On-Off-On" and "On-Off" fluorescent switching. The self-assembly of two Cu^{2+} ions and two molecules of fluoroionophore **1** to form closed structure $[Cu_2(L)_2]^{4+}$ seems to be responsible for nanomolar sensitivity towards Cu^{2+}. The combination of delayed second protonation of **1** (pK_{a2}=2.6) and stepwise protonation of $[Cu_2\mathbf{L}_2]^{4+}$ causes unusual stability of $[Cu(\mathbf{L}H)_2]^{4+}$ even at pH<2.

Keywords Chemosensor · 8-hydroxyquinoline · Cu^{2+} · Co^{2+} · Fluorescence quenching · pH stability

Introduction

Fluorescence signaling systems can be designed for signal transduction upon analyte binding offering possibilities to use them as chemical sensors in biomedical research and as chemical logics for molecular information processing [1–5]. Although up to now various analytical tools such as GC-MS, ion-mobility spectroscopy (IMS), electrochemical detection, to name a few, are available for the detection of metal ions but these methods cannot be used in field due to their limited portability, lack of selectivity and sensitivity to interfering analytes and high cost. In this context, fluorescence based assays provide advantages due to their high sensitivity, specificity, potential for portability and real time monitoring with fast response time.

For last few years, research has focused on developing fluorescent sensors as a safeguard for global ecosystem, for monitoring of toxic and carcinogenic metals such as Pb^{2+}, Hg^{2+}, Cu^{2+}, Cd^{2+}, Co^{2+} and Zn^{2+} that impose serious human and environmental health hazards [1–5]. Copper plays role in diverse and increasing number of pathways, involving physiological and disease processes. So, despite being an essential element in biological systems, Cu^{2+} has a toxic impact on the microorganisms at even sub-micromolar concentrations [6, 7] and is harmful to human at higher concentrations being associated with Alzheimer's, Prion and Wilson's disease etc. [8, 9]. Cobalt is another essential trace element found in Vitamin B_{12} and other metalloproteins. Cobalt is released in the environment from industries, volcanic eruption, truck and airplane exhaust, forest fire, soil and dust. The maximum dietary tolerable level of cobalt for common livestock species is 10 ppm. Exposure to high level of cobalt can cause heart diseases, vasodilation, thyroid enlargement and cancer [10, 11].

A variety of fluorescent sensors of Cu^{2+} exhibiting either 'on-off'/'off-on' or ratiometric signaling have been developed [1–5, 12, 13]. In nature, blue copper proteins such as rusticyanin possess the four ligating atoms (2 × N + 2 × S) arranged around Cu^{2+} in a distorted tetrahedral arrangement but have high acid stability as the copper binding site is located within a hydrophobic region at one end of the molecule, surrounded by a number of aromatic rings and hydrophobic residues. This conformation probably contributes to the acid stability of the copper site, since the close association of aromatic rings with the histidine ligand sterically hinders

P. Singh (✉) · R. Kumar · S. Kumar (✉)
Department of Chemistry, UGC Centre for Advanced Studies, Guru Nanak Dev University, Amritsar 143005, India
e-mail: prabhpreet.chem@gndu.ac.in
e-mail: subodh_gndu@yahoo.co.in

their dissociation from copper [14–16]. In this context, to achieve Cu^{2+} sensitivity and selectivity, the potential of mixed ligating sites (S, N, O or S, N), as prevalent in nature are more interesting.

In light of our previous results on anthracene based receptors, the placement of anthracene ring either at the backbone of the fluoroionophore as in **I** [17] or at the terminal of the fluoroionophore as in **II** [18] remarkably affects their photophysical behavior on addition of Cu^{2+}.

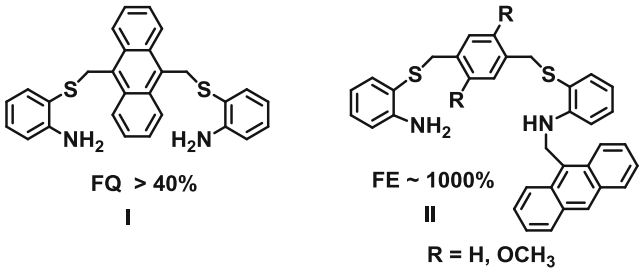

In case of **I**, anthracene ring strongly participates in cation-π (Cu^{2+}–anthracene) interactions and results in fluorescence quenching with Cu^{2+}. However in case of **II**, the shift of anthracene from backbone to the terminal of the fluoroionophore, reduces the participation of anthracene ring in cation-π interaction and thus leads to selective fluorescence enhancement with Cu^{2+}. Unfortunately, **II** shows lower complexation constants towards Cu^{2+}, leading to increased interference by other metal ions. We envisaged that the presence of stronger co-ordinating groups at 9 and 10 positions of anthracene moiety will provide better coordination towards Cu^{2+} and as a result the participation of anthracene ring in stabilization of Cu^{2+} complex would be decreased. So, we have realized this design through synthesis of fluoroionophores **1** and **2** based on 8-hydroxyquinoline (8-HQ) subunits. 8-HQ and its derivatives [19] possess good photostability and strong ability to complex metal ions and are used in organic light emitting diode devices [20], in chromatography [21] and in electrochemiluminescence [22] etc. Recently, 8-HQ based fluoroionophores have been developed for detecting Cd^{2+}, Hg^{2+}, Zn^{2+} ions and have proved to be effective in discriminating Cd^{2+} over Zn^{2+} [23, 24]. However, use of 8-hydroxyquinoline based chemosensors for the detection of the Cu^{2+} and Co^{2+} has been scarcely studied [25–27].

In this report we have shown that fluoroionophore **1**, which possesses strong coordinating groups at 9,10 positions of anthracene, provides better coordination towards Cu^{2+} and can be used for the nanomolar estimation of Cu^{2+} under elevated concentration of other metal ions. Due to increased number of aryl rings in fluoroionophore **1**, it shows increased hydrophobic character and acts as ditopic receptor in which one 8-alkoxyquinoline unit undergoes normal protonation but the second quinoline unit undergoes delayed protonation at significantly lower pH. This scenario provides the opportunity to make supramolecular complex even at pH<2. The lowering in emission either by binding Cu^{2+} or H^{+} or both resulted in NOR logic gate with low output at 424 nm and "On-Off-On" and "On-Off" fluorescent switching phenomena.

Experimental

General

Melting points were determined in capillaries and are uncorrected. ^{1}H NMR spectra were recorded on JEOL Al 300 MHz instrument using $CDCl_3$ solution containing tetramethylsilane as an internal standard. The chemical shifts are reported in δ values relative to TMS and coupling constants (J) are expressed in Hertz. ^{13}C NMR spectra were recorded at 75 MHz and the values are reported relative to $CDCl_3$ signal at δ 77.0. Chromatography was performed with silica gel 100–200 mesh and the reactions were monitored by thin layer chromatography (TLC) with glass plates coated with silica gel HF-254. 9,10-Bis(chloromethyl)anthracene [28], and 9-(chloromethyl)anthracene were prepared according to the literature procedures. The pH measurement were made using EQUIP-TRONIC, EQ-611 pH meter equipped with glass electrode. The fluorescence spectra were recorded by excitation at 345 nm at RF-1501 spectrofluorophotometer from Shimadzu and absorption spectra were recorded at UV-1601 spectrophotometer from Shimadzu. The pH titration of **1/2** and **1**-Cu(II) complex were performed with acid (HCl) to investigate the <7 pH range and in a separate experiment with base (NaOH) to investigate the >7 pH range and at regular interval of pH fluorescence spectrum were recorded. Solutions containing **1** and **2** (3 μM) and various concentrations of metal nitrates (0.15 μM to 300 μM) were prepared in CH_3CN: H_2O (4:1 v/v) at pH 7 (HEPES 10 mM) separately in 10 ml measuring flasks. For interference evaluation, the solutions containing **1** and **2** (3 μM), one of the interfering metal nitrates [Co^{2+}, Ni^{2+}, Cd^{2+}, Zn^{2+}, Ag^{+}, Hg^{2+}, Cr^{3+}, Fe^{3+}, Pb^{2+} (150 μM)] and (0.6, 1.2, 1.8, 2.4, 3.0, and 6.0 μM) of copper nitrate in CH_3CN:H_2O (4:1 v/v) at pH 7 (HEPES 10 mM) were prepared. The solutions were kept at 25±1 °C for 3 h and were shaken occasionally. Solutions containing **1** (30 μM) and various concentrations of copper nitrate (3 μM to 300 μM) were prepared in CH_3CN:H_2O (4:1) separately in 10 ml measuring flasks. The solutions were kept at 25±1 °C for 3 h and were shaken occasionally. All absorption and fluorescence scans were saved as ACS II files and further processed in Excel™ to produce all graphs shown. The spectral data were analyzed through curve fitting procedures by using non-linear regression analysis programme SPECFIT 3.0.36 to determine the protonation constants, stability constants and the distribution of various species.

Synthesis of Fluoroionophore 1

In a round bottomed flask, pre-washed NaH (110 mg, 4.6 mmol) was taken in dry DMF and 8-hydroxyquinoline (**4**) (365 mg, 2.5 mmol) was added with stirring at 80±2 °C. After the hydrogen evolution ceased, TBA HSO_4 (25–30 mg) and 9,10-bis(chloromethyl)anthracene (**3**) (300 mg, 1.1 mmol) were added and stirring was continued for 24 h. During this period reaction was completed. The suspended solid was filtered off and was washed with ethyl acetate. The combined filtrate was distilled off under vacuum and the residue was column chromatographed over silica gel to isolate **1** (Scheme 1), which was further crystallized from dichloromethane, yield 30 %, yellow solid, m.p. 234–235 °C (CH_2Cl_2), HRMS *m/z* 493 ($M^+ + H$); ^1H NMR (DMSO-d_6 - TFA): δ 6.22 (s, 4H, OCH_2), 7.36 (d, J=6.9 Hz, 4H, Anth-H), 7.68 (d, J =7.5 Hz, 2H, HQH-7), 7.72–7.86 (m, 6H, HQH-3,5, 6), 8.18 (d, J=6.9 Hz, 4H, Anth-H), 8.50 (d, J=4.8 Hz, 2H, HQH-4), 8.84 (d, J=8.4 Hz, 2H, HQH-2)ppm; ^{13}C NMR (DMSO-d_6–TFA): δ 66.53, 116.50, 123.00, 124.70, 126.76, 129.38, 130.50, 131.81, 132.68, 133.38, 133.50, 145.52, 149.78, 151.25 ppm. (Found C, 82.70; H, 4.74; N, 5.43 % $C_{34}H_{24}N_2O_2$ requires C, 82.91; H, 4.91; N, 5.69 %).

Synthesis of Fluoroionophore 2

In a round bottomed flask, pre-washed NaH (132 mg, 5.5 mmol) was taken in dry DMF and 8-hydroxyquinoline (**4**) (400 mg, 2.75 mmol) was added with stirring at 80± 2 °C. After the hydrogen evolution ceased, TBA HSO_4 (25–30 mg) and 9-(chloromethyl)anthracene (**5**) (561 mg, 2.48 mmol) were added and stirring was continued for 24 h. During this period reaction was completed. The suspended solid was filtered off and was washed with ethyl acetate. The combined filtrate was distilled off under vacuum and the residue was column chromatographed over silica gel to isolate **2** (Scheme 1), which was further crystallized from dichloromethane, yield 20 %, m.p. 123–125 °C (CH_2Cl_2), HRMS *m/z* 336 ($M^+ + H$); ^1H NMR ($CDCl_3$): δ 6.26 (s, 2H, OCH_2), 7.39 (dd, J_1=8.4 Hz, J_2=4.2 Hz, 1H, HQH-3), 7.43–7.54 (m, 7H, Anth-H, HQH-5, 6, 7), 8.03 (d, J_1=7.5 Hz, 2H, Anth-H), 8.14 (dd, J_1=8.4 Hz, J_2=1.8 Hz, 1H, HQH-4), 8.42 (d, J=8.7 Hz, 2H, Anth-H), 8.52 (s, 1H, Anth-H), 8.88 (dd, J_1=4.2 Hz, J_2= 1.8 Hz, 1H, HQH-2) ppm; ^{13}C NMR ($CDCl_3$): δ 64.37, 110.49, 120.42, 121.53, 124.22, 124.95, 126.43, 126.66, 126.76, 129.00, 129.58, 131.44, 131.49, 135.93, 140.59, 149.29, 155.07 ppm. (Found C, 85.65; H, 4.92; N, 4.01 % $C_{24}H_{17}NO$ requires C, 85.94; H, 5.11; N, 4.18 %).

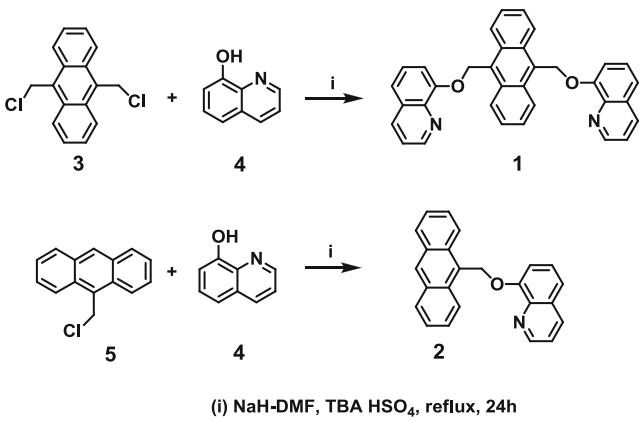

Scheme 1 Synthesis of fluoroionophores 1 and 2

Results and Discussion

The solutions of fluoroionophores **1** and **2** (30 μM) in CH_3CN:H_2O (4:1 v/v), in their UV-visible spectra displayed λ_{max} at 397, 376 and a shoulder at 357 nm typical for anthracene unit. The solutions of **1** and **2** (3 μM) [CH_3CN-H_2O (4:1)] on excitation at λ_{ex} 345 nm gave fluorescence spectra with maxima at λ_{max} 402, 424 nm and a shoulder at 449 nm due to anthracene unit [29, 30]. Since both anthracene and 8-hydroxyquinoline emit between 300 and 450 nm region, the observed emission may have contribution due to both anthracene and 8-hydroxyquinoline fluorophores. In concentration range 1–100 μM, the fluorescence intensity of **1** and **2** increased linearly with the increase in concentration and indicates that these fluoroionophores are not susceptible to self-quenching or to the aggregation process at least between 1 and 100 μM concentrations.

Behavior of Fluoroionophores 1 and 2 Towards pH of Medium

Before studying the complexation with different cations, we studied the pH dependence of the fluorescence spectrum of fluoroionophores **1** and **2** [31]. The fluorescence intensity of **1** (1 μM, CH_3CN:H_2O, 4:1, v/v) remained unaffected between pH 11 and 7.0 and on further lowering of pH, fluoroionophore **1** underwent fluorescence quenching in a stepwise manner (Fig. 1).

The lowering of pH from 7.0 to 5.9 resulted in ~10 % decrease in the fluorescence intensity and then remained stable between pH 5.9 and 4.0. Further lowering of pH from 4.0 to 1.0 resulted in sharp decrease (>80 %) in the fluorescence intensity with simultaneous appearance of a new emission band at 490 nm (Figs. 1 and 2). The intensity of 490 nm emission band increased up to pH 2.0 and then on further lowering of pH, it decreased. From the spectral fitting of the fluorescence data for pH titration using non-linear regression analysis (SPECFIT-32), three consecutive protonation steps are observed for **1** that we ascribe to the formation of HL^+ (pKa_1=6.7±0.1) due to protonation of nitrogen of first quinoline; H_2L^{2+} (pKa_2=2.6±0.1) due to protonation of nitrogen of second

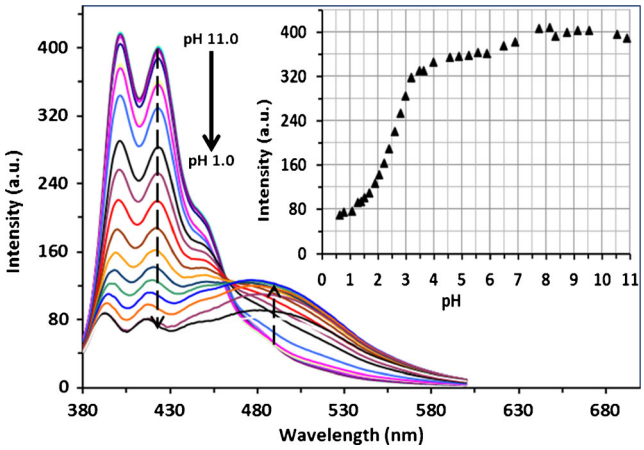

Fig. 1 The effect of pH on the fluorescence spectrum of **1** (1 μM) recorded in CH_3CN:H_2O (4:1, v/v) at 25±1 °C; λ_{ex}=345 nm. [Inset] The plot of gradual change in fluorescence intensity of **1** (1 μM) taken at 423 nm vs. change in pH of the solution

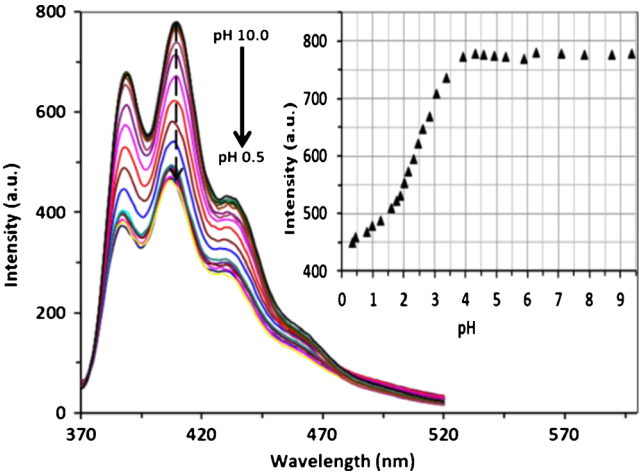

Fig. 3 The effect of pH on the fluorescence spectrum of **2** (1 μM) recorded in CH_3CN:H_2O (4:1, v/v) at 25±1 °C; λ_{ex}=345 nm. [Inset] The plot of gradual change in fluorescence intensity of **2** (1 μM) taken at 423 nm vs. change in pH of the solution

quinoline; and H_3L^{3+} (pKa_3=1.0±0.1) probably diprotonated species under strong acidic conditions (pH<1) undergoes further protonation at etheral oxygen. In this respect fluoroionophore **1** behaves as pH sensor between pH 4 and 1.0 with "ON-OFF" system when monitored at 400 nm and as "OFF-ON" system when monitored at 490 nm.

Similarly, fluoroionophore **2** (1 μM, CH_3CN:H_2O, 4:1, v/v) on pH titration shows that fluorescence remains unaffected between pH 10 and 4.0 and then decreases sharply between pH 4.0 and 1.0 (Fig. 3). The spectral fitting of data shows pK_a=2.4±0.1.

Therefore, the proximity of 8-hydroxyquinoline moiety with anthracene tenders quinoline nitrogen less basic with pKa=2.6±0.1 and pKa=2.4±0.1 for fluoroionophores **1** and **2**, respectively and also allows the protonation of two quinoline units in fluoroionophore **1** to proceed in a stepwise manner.

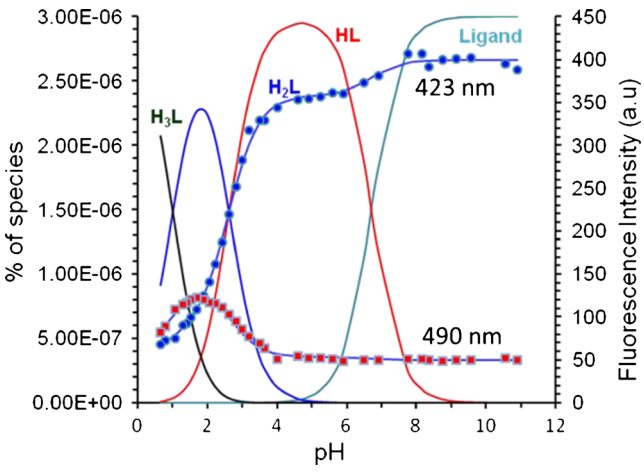

Fig. 2 pH titration curve for **1** (1 μM, λ_{ex}=345 nm) at λ_{em} 423 and 490 nm superimposed on the % distribution of the various species. Right hand axis shows the fluorescence intensity whereas left hand axis shows the % distribution of different species at different pH values ranging from 11 to 1

This could be attributed to the ICT from quinoline to anthracene unit which makes the nitrogen lone pair less available and so less basic also. It is noteworthy that quinoline based multipodal benzene systems earlier reported by our group–dipod, tripod and tetrapod [32, 33] in CH_3CN:H_2O show single step protonation with log β_{HL}=4.21±0.2 and respective stepwise protonation is not observed. The formation of emission band at 490 nm could be attributed to the intramolecular interaction of the two pendent quinoline moieties and is further supported by the lack of 490 nm emission in case of fluoroionophore **2**.

Interactions of Fluoroionophores 1 and 2 Towards Metal Ions

In the preliminary fluorescence studies, transition metal ions Ag^+, Cr^{3+}, Pb^{2+}, Ni^{2+} Hg^{2+} and Zn^{2+} (30 μM), did not modulate the fluorescence intensity of fluoroionophore **1** (3 μM, CH_3CN:HEPES buffer (4:1; v/v), pH 7.1) and the decrease in fluorescence intensity was observed for Co^{2+} (~70 %) and Cd^{2+}, Fe^{3+} (~40 %) at 30 μM. However, on addition of even 3 μM Cu^{2+} to the solution of **1**, a dramatic decrease in the fluorescence intensity (~80 %) was observed. These preliminary results clearly show that **1** strongly binds with Cu^{2+} and induces fluorescence quenching.

The titration of fluoroionophore **1** (3 μM, HEPES buffered CH_3CN:H_2O (4:1 v/v), pH 7.1) with Cu^{2+} showed that upon gradual addition of Cu^{2+} between 0.05 and 1.0 equiv (0.15–3 μM) of **1**, the fluorescence intensity decreased gradually in a linear manner between 0 and 3 μM concentration of Cu^{2+} and then a plateau was achieved (Fig. 4). The non-linear regression analysis of these titration data shows the formation of 2:2 Cu^{2+}-**1** complex with log β_{M2L2}=19.36±0.1. In order to further conspicuously determine the stoichiometry of **1**-Cu^{2+} complex, the **1**-Cu^{2+} complex was obtained by dissolving Cu^{2+}

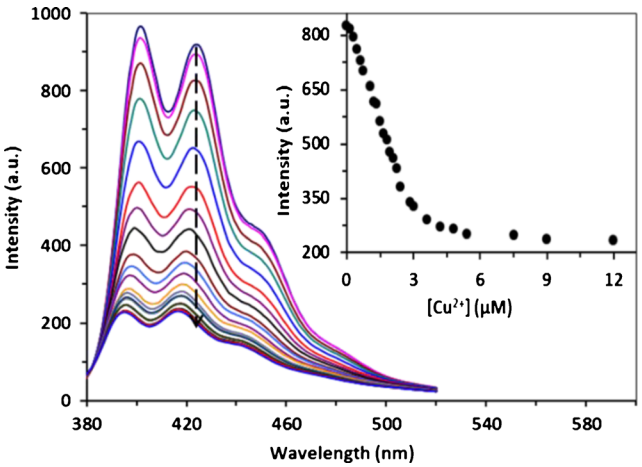

Fig. 4 Fluorescence spectra of **1** (3 μM) recorded in pH 7.1 HEPES buffered $CH_3CN:H_2O$ (4:1 v/v) solution on addition of the Cu^{2+} ions (0–24 μM, 0–8 equiv). Excitation at 345 nm. [Inset] The plot of change in fluorescence intensity of **1** (3 μM) taken at 420 nm vs. gradual change in concentration of Cu^{2+}

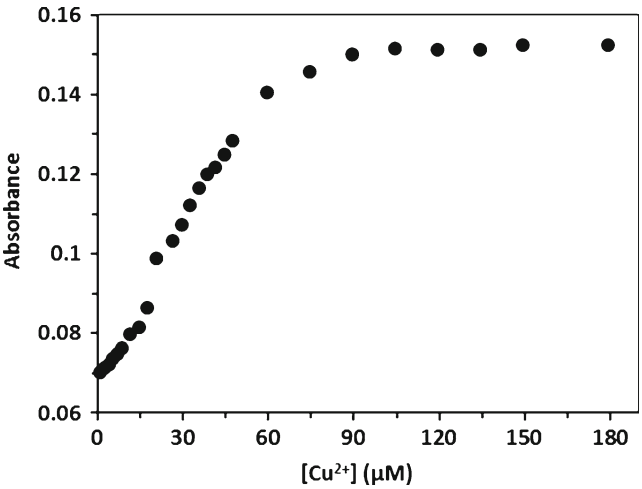

Fig. 5 The change in absorbance of **1** (30 μM, HEPES buffered $CH_3CN:H_2O$ (4:1 v/v) pH 7.1) vs. concentration of Cu^{2+}

and **1** in a 1:1 ratio under same solvent conditions as used in fluorescence studies followed by slow evaporation of the solvent and its high resolution mass spectrum was recorded. The peaks obtained at *m/z* unit of 1110.6964 and 1047.3894 could be assigned to a species corresponding to $[2L+2Cu^{2+}]$ and $[2L+Cu^{2+}]$, respectively. The presence of a peak at *m/z* unit of 493.2008 is likely to be due to free fluoroionophore **1**. The fluorescence quantum yield of fluoroionophore decreased from 0.105 to 0.021 in the presence of 3 μM Cu^{2+}. The lowest concentration of Cu^{2+} to be detected constitutes 150 nM. Significantly, the titrations of **1** with other metal ions viz., Ag^{+}, Cr^{3+} and Pb^{2+} show log β<3.

To explore further the potential of fluoroionophore **1** to act also as a chromogenic sensor and the role of the anthracene moiety in π-cation interactions, the effect of Cu^{2+} on the UV–Vis behavior of **1** was studied. The plot of titration of **1** (30 μM, CH_3CN:HEPES buffer (4:1), pH 7.1) with Cu^{2+} ions showed a gradual increase in absorption (extinction coefficient) (Fig. 5) when measured at 401 nm over a Cu^{2+} concentration range of 1.5–60 μM (0.05–2 eq), above which absorbance trailed to small residual value and plateau was achieved. The increase in absorbance of the anthracene unit on addition of Cu^{2+} rules out any Cu^{2+}-anthracene interaction.

Since fluoroionophore **1** in its preliminary studies was also showing fluorescence quenching with Co^{2+}, Cd^{2+}, Hg^{2+}, Fe^{3+} and Zn^{2+} at elevated levels, the fluoroionophore **1** may have the ability to analyze these metals. The fluorescence intensity of fluoroionophore **1** (3 μM) showed a gradual decrease in fluorescence between 0 and 10 μM of Co^{2+} and can be used to measure Co^{2+} 600 nM as lowest detection limit (Fig. 6). The stoichiometry of complexation for **1**-Co^{2+} was determined through SPECFIT with log β_{ML}=7.21±0.2; log β_{M2L}=11.42±0.2 (Table 1). Similarly, fluorescence intensity of fluoroionophore **1** (3 μM) showed a gradual decrease in fluorescence on gradual addition of Cd^{2+} between 0 to 150 μM and Fe^{3+} between 0 to 300 μM, in a separate titration experiments and then a plateau was reached (Fig. 6). The determination of stability constants gives log β_{ML}=5.28±0.02; log β_{M2L}=10.2±0.08 for **1**-Cd^{2+} complex and log β_{ML}=5.9±0.02; log β_{M2L}=10.5±0.08 for **1**-Fe^{3+} complex, respectively.

Therefore, fluoroionophore **1** shows higher senstivity towards Cu^{2+} as compared to other interfering ions. The log β values for other metal ions are too small and could not be determined. Therefore, the fluoroionophore **1** has far more sensitivity and selectivity for Cu^{2+} as compared to other metal ions, however only in case of Co^{2+}, fluoroionophore **1** lost selectivity but still possesses more sensitivity.

The titration of fluoroionophore **2** (3 μM) with Cu^{2+} showed gradual decrease in fluorescence between 0 and 3 μM and then

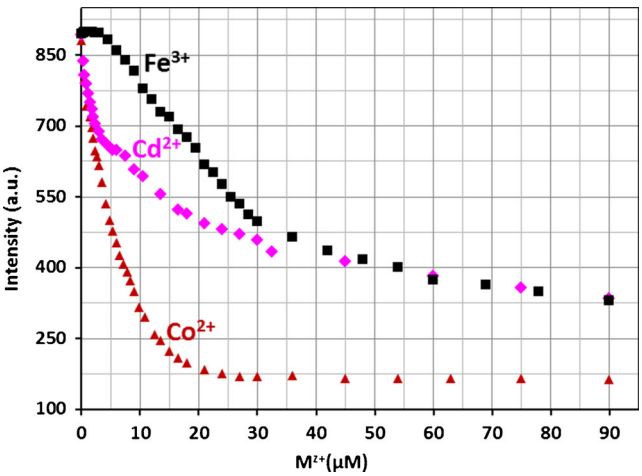

Fig. 6 Combined plot shows the effect of various metal ions on the fluorescence intensity of **1** (3 μM) recorded in HEPES buffered $CH_3CN:H_2O$ (4:1 v/v), pH 7.1; (▲) Co^{2+}; (♦) Cd^{2+}; (*black square*) Fe^{3+}

Table 1 The stability constants of fluoroionophore 1 with various metal ions

Sr. No.	Metal ion	FQ	M_2L_2	ML	M_2L
1.	Cu^{2+}	"ON-OFF"	19.4±0.1		
2.	Co^{2+}	"ON-OFF"		7.0±0.2	11.4±0.2
3.	Cd^{2+}	"ON-OFF"		5.3±0.02	10.2±0.08
4.	Fe^{3+}	"ON-OFF"		5.9±0.02	10.5±0.08
5.	Zn^{2+}	"ON-OFF"		4.4±0.02	8.6±0.1
6.	Pb^{2+}	"ON-OFF"		<3	
7.	Cr^{3+}			<2	
8.	Ag^{+}			<2	

plateau was achieved (Fig. 7). The spectral fitting of the data shows the formation of only 1:1 (ML) complex with log β=6.96±0.1. It is well documented that when Cu^{2+} binds tightly to the host compound, intracomplex quenching takes place via *energy* or *electron* transfer.

Interference and Anion Displacement Studies

Although other metal ions individually do not exhibit any significant quenching but to further evaluate the selectivity of fluoroionophore **1** towards Cu^{2+}, the titration of **1** with Cu^{2+} in the presence of probable interfering metal ions was carried out. The solutions containing **1** (3 μM), one of the metal ions Ag^{+}, Cd^{2+}, Co^{2+}, Zn^{2+}, Hg^{2+}, Pb^{2+}, Cr^{3+}, Fe^{3+} and Ni^{2+} (300 μM) and varied concentration of Cu^{2+} (0.6, 1.2, 1.8, 2.4, 3, 6 μM) were prepared separately in HEPES buffered CH_3CN:H_2O (4:1 v/v), pH 7.1 and their fluorescence spectra were recorded. The fluorescence of **1** containing only Cu^{2+} was also recorded for comparison. The plot of fluorescence

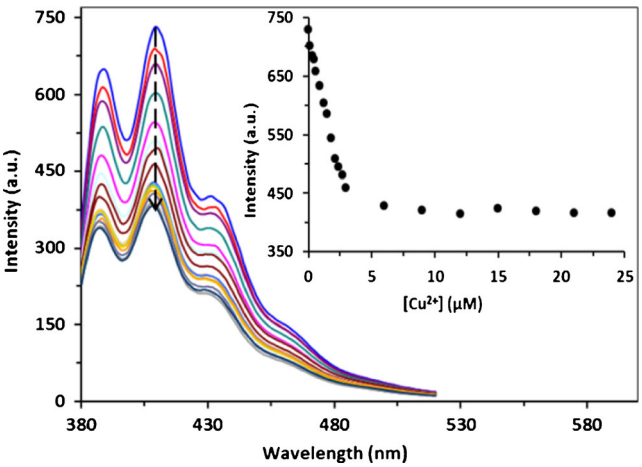

Fig. 7 Fluorescence spectra of **2** (3 μM) recorded in pH 7.1 HEPES buffered CH_3CN:H_2O (4:1 v/v) solution on addition of the Cu^{2+} ions (0–24 μM, 0–8 equiv). Excitation at 345 nm. [Inset] The plot of change in fluorescence intensity of **2** (3 μM) taken at 420 nm vs. gradual change in concentration of Cu^{2+}

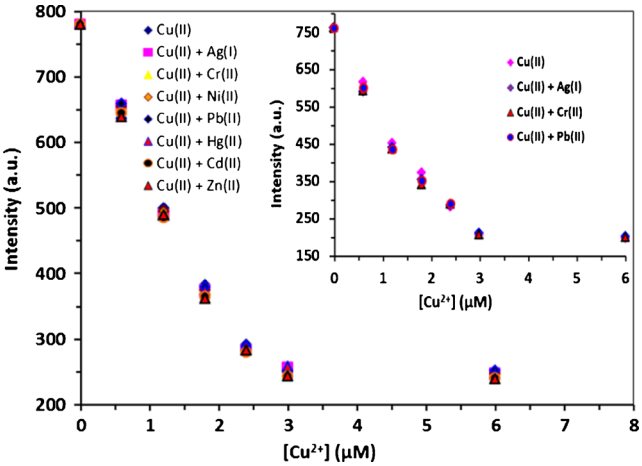

Fig. 8 Estimation of Cu^{2+} in the presence of various metal ions (15 μM) recorded in pH 7.1 HEPES buffered CH_3CN:H_2O (4:1 v/v) solution. [Inset] Estimation of Cu^{2+} in the presence of various metal ions (300 μM) recorded in pH 7.1 HEPES buffered CH_3CN:H_2O (4:1 v/v) solution

intensity of **1**-Cu^{2+} and **1**-Cu^{2+}-M^{z+} solutions vs. Cu^{2+} concentration shows that the presence of Ag^{+}, Pb^{2+} and Cr^{3+} (300 μM) and Cd^{2+}, Zn^{2+}, Ni^{2+} and Hg^{2+} (15 μM) does not interfere in the estimation of Cu^{2+} (Fig. 8). The Co^{2+} does interfere in the estimation of Cu^{2+}. Therefore, **1** can estimate 0.15–3 μM of Cu^{2+} through fluorescence spectroscopy whilst Cr^{3+}, Ag^{+} and Pb^{2+} (300 μM) do not interfere (Fig. 8).

Anions are important part of our biological system and at elevated concentration prove fatal to human body. It is known that pyrophosphate and cyanide have strong affinity towards Cu^{2+} and their presence in solution of **1** can disrupt the estimation of Cu^{2+}. In fact fluorophore-Cu^{2+} complexes have been used for the detection of cyanide and phosphate ions via displacement assay approach [34, 35]. In case of **1**-Cu^{2+} complex, the addition of cyanide or phosphate caused no

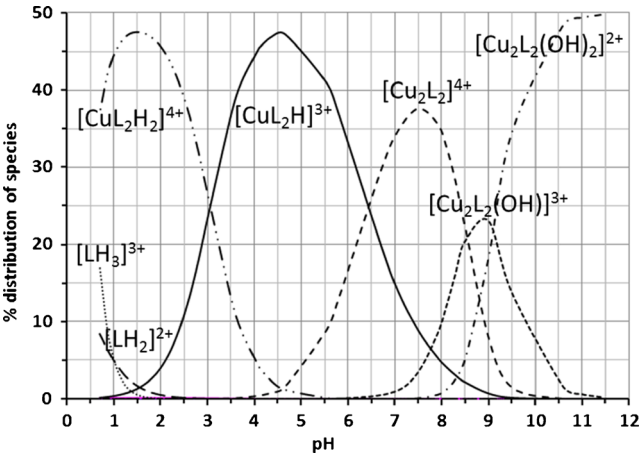

Fig. 9 Distribution of species vs. pH for **1**-Cu^{2+} (1:1) solution (L=**1**) in CH_3CN:H_2O (4:1 v/v). The species corresponding to each curve are indicated

Table 2 Stepwise protonation constants of M_2L_2 [1-Cu(II)] complex observed in pH titration

Equilibrium	Log β
$2L + Cu^{2+} + 2H^{+} \rightleftharpoons [Cu(LH)_2]^{4+}$	30.26±0.15
$2L + Cu^{2+} + H^{+} \rightleftharpoons [CuL(LH)]^{3+}$	27.20±0.17
$2L + 2Cu^{2+} \rightleftharpoons [Cu_2L_2]^{4+}$	26.91±0.18
$2L + 2Cu^{2+} + H_2O \rightleftharpoons [Cu_2L_2(OH)]^{3+} + H^{+}$	18.37±0.31
$2L + 2Cu^{2+} + 2H_2O \rightleftharpoons [Cu_2L_2(OH)_2]^{2+} + 2H^{+}$	9.26±0.25

change in their fluorescence intensity. These results clearly indicate that Cu^{2+} binds strongly with the fluoroionophore **1** and CN^{-}, PO_4^{2-} do not interfere in the estimation of Cu^{2+}.

Stability of 1-Cu^{2+} Complex at Low pH

In order to evaluate the usability of fluoroionophore **1** under different pH conditions, the fluorescence of 1:1 solution of **1** and Cu^{2+} was determined at different pH values. The results are summarized in Fig. 9 and list of the different species with relevant stability constants are reported in Table 2. Figure 9 shows that at pH >10, a closed structure with 2:2 stoichiometry i.e. $[Cu_2L_2(OH)_2]^{2+}$ (L =**1**) is formed which on lowering the pH undergoes stepwise protonation to form $[Cu_2L_2(OH)]^{3+}$ and $[Cu_2L_2]^{4+}$ complexes. On lowering the pH to <7, the protonation at quinoline nitrogen leads to release of one Cu^{2+} and results in formation of $[Cu(L)(LH)]^{3+}$ complex, which is the major complex at pH~5.0 and is in consonance with first pK_a value of the quinoline moiety. On lowering the pH from 4, the protonation of the quinoline nitrogen of the second molecule of **1** in the complex takes place and leads to formation of $[Cu(LH)_2]^{4+}$ complex (Fig. 10). The formation of $[Cu(LH)_2]^{4+}$ complex is completed at pH as low as 1.4 which is quite near to pK_{a2} (2.4±0.1) of the free fluoroionophore **1**. Such stability of Cu^{2+} complexes at low pH is quite un-common. It is further noteworthy that when $[Cu(\mathbf{1})]^{2+}$ (1:1) species was included in the hypothesized set of species present in the solution for the fluorescence data refinement for complex pH titration, the SPECFIT data processing discarded it, excluding its presence. Therefore, the combination of hydrophobic character of the aromatic rings along with the presence of ligating sites which accept the protons leads to stability of $[Cu(LH)_2]^{4+}$ complex even at pH 1.0.

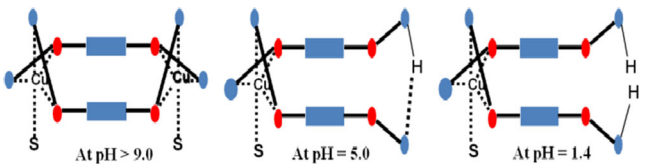

Fig. 10 The proposed model representation of the major species formed in the pH titration of **1**-Cu(II) complex

In this pH titration of the complex, the formation of excimer band at 490 nm for complex species $[CuL_2H_2]^{4+}$, ascribed to intramolecular π-stacking involving two 8-hydroxyquinoline moieties in the excited state, was observed. At pH <1, the formation of $[LH_2]^{2+}$ and $[LH_3]^{3+}$ species was observed which is consonance with pH titration of free **1**.

Conclusions

Fluoroionophore **1** can selectively estimate Cu^{2+} between 150 nM and 3 μM even in the presence of elevated levels of Ag^{+}, Cr^{3+} and Pb^{2+} (300 μM) and Cd^{2+}, Zn^{2+}, Ni^{2+} and Hg^{2+} (15 μM). The presence of strong binding anions such as cyanide and phosphate does not interfere in the estimation of Cu^{2+}. The self-assembly of two Cu^{2+} ions and two molecules of **1** to form the closed structure $[Cu_2(L)_2]^{4+}$ seems to be responsible for its nanomolar sensitivity towards Cu^{2+}.

Acknowledgments We thank UGC, New Delhi for CAS and UPE programmes; DST, New Delhi for financial assistance and FIST programme.

References

1. Kaur K, Saini R, Kumar A, Luxami V, Kaur N, Singh P, Kumar S (2010) Coord Chem Rev 256:1992–2028
2. Kaur N, Kumar S (2011) Tetrahedron 67:9233–9264
3. Formica M, Fusi V, Giorgi L, Micheloni M (2012) Coord Chem Rev 256:170–192
4. Jeong Y, Yoon J (2012) Inorg Chim Acta 381:2–14
5. Zhang JF, Zhou Y, Yoon J, Kim JS (2011) Chem Soc Rev 40:3416–3429
6. Stern BR (2010) J Toxicol Environ Health A Curr Issues 73:114–127
7. Crisponi G, Nurchi VM, Fanni D, Gerosa C, Nemolato S, Faa G (2010) Coord Chem Rev 254:876–889
8. Viles JH (2012) Coord Chem Rev 256:2271–2284
9. Kozlowski H, Luczkowski M, Remelli M, Valensin D (2012) Coord Chem Rev 256:2129–2141
10. Okamoto S, Eltis LD (2011) Metallomics 3:963–970
11. Simonsen LO, Harbak H, Bennekou P (2012) Sci Total Environ 432:210–215
12. Bencini A, Bernardo MA, Bianchi A, Garcia-Espana E, Giorgi C, Luis S, Pina F, Valtancoli B (2002) Adv Supramol Chem 8:79–130
13. Dutta M, Das D (2012) TrAC Trends Anal Chem 32:113–132
14. Warren JJ, Lancaster KM, Richards JH, Gray HB (2012) J Inorg Biochem 115:119–126
15. Solomon EI, Hadt RG (2011) Coord Chem Rev 255:774–789
16. Farver O, Pecht I (2011) Coord Chem Rev 255:757–773
17. Kaur S, Kumar S (2004) Tetrahedron Lett 45:5081–5085
18. Kumar S, Singh P, Kaur S (2007) Tetrahedron 63:11724–11732
19. Albrecht M, Fiege M, Osetska O (2008) Coord Chem Rev 252:812–824
20. Thejo KN, Dhoble SJ (2012) Renew Sustain Energy Rev 16:2696–2723
21. Tria J, Butler ECV, Haddad PR, Bowie AR (2007) Anal Chim Acta 588:153–165

22. Muegge BD, Brooks S, Richter MM (2003) Anal Chem 75:1102–1105
23. Mameli M, Aragoni MC, Arca M, Caltagirone C, Demartin F, Farruggia G, Filippo GD, Devillanova FA, Garau A, Isaia F, Lippolis V, Murgia S, Prodi L, Pintus A, Zaccheroni NA (2010) Chem Eur J 16:919–930
24. Tang XL, Peng XH, Dou W, Mao J, Zheng JR, Qin WW, Liu WS, Chang J, Yao XJ (2008) Org Lett 10:3653–3656
25. Zhu H, Fan J, Lu J, Hu M, Cao J, Wang J, Li H, Liu X, Peng X (2012) Talanta 93:55–61
26. Park JS, Jeong S, Dho S, Lee M, Song C (2010) Dyes Pigments 87: 49–54
27. Mei Y, Bentley PA, Wang W (2006) Tetrahedron Lett 47:2447–2449
28. Miller MW, Amidon RW, Tawney PO (1955) J Am Chem Soc 77: 2845–2848
29. Birks JB (1970) Photophysics of aromatic molecules. Wiley-interscience, New York
30. Rdrigeuz L, Alves S, Lima JC, Parola AJ, Pina F, Soriano C, Albelda T, Garcia-Espana E (2003) J Photochem Photobiol A Chem 159:253–258
31. Bencini A, Berni E, Bianchi A, Fornasari P, Giorgi C, Lima JC, Lodeiro C, Melo MJ, de Melo SJ, Parola AJ, Pina F, Pina J, Valtancoli B (2004) Dalton Trans 2180–2187
32. Singh P, Kumar S (2007) 8-hydroxyquinoline based multipodal system: effect of spatial placement of 8-hydroxyquinoline on metal ion recognition. J Incl Phenom Macrocycl Chem 58:89–94
33. Kumar S, Kaur S, Singh G (2003) Supramol Chem 15:65–67
34. Tetilla MA, Aragoni MC, Arca CMC, Bazzicalupi C, Bencini A, Garau A, Isaia F, Laguna A, Lippolis V, Meli V (2011) Chem Commun 47: 3805–3807
35. Wang J, Ha CS (2010) Tetrahedron 66:1846–1851